Geophysical Research Letters

RESEARCH LETTER
10.1029/2023GL103323

A Spectral Analysis of Near-Surface Mean Wind Speed and Gusts Over the Iberian Peninsula

Eduardo Utrabo-Carazo[1], Cesar Azorin-Molina[1], Enric Aguilar[2], and Manola Brunet[2]

[1]Centro de Investigaciones sobre Desertificación, Consejo Superior de Investigaciones Científicas (CIDE, CSIC-UV-Generalitat Valenciana), Climate, Atmosphere and Ocean Laboratory (Climatoc-Lab), Moncada, Spain, [2]Centre for Climate Change, Universitat Rovira i Virgili, Tarragona, Spain

Key Points:

- Surface winds correlate with the stratospheric polar vortex in periods close to 1 year, with a 2–3 months lag with respect to the anti-phase
- Surface mean wind speed and gusts are decoupled for periods between 9 and 11 years, being greater in summer and disappearing in winter
- Spectral analysis showed differences between observed and ERA5-Land reanalysis surface winds

Supporting Information:

Supporting Information may be found in the online version of this article.

Correspondence to:

E. Utrabo-Carazo,
eduardo.utrabo@ext.uv.es

Citation:

Utrabo-Carazo, E., Azorin-Molina, C., Aguilar, E., & Brunet, M. (2023). A spectral analysis of near-surface mean wind speed and gusts over the Iberian Peninsula. *Geophysical Research Letters*, *50*, e2023GL103323. https://doi.org/10.1029/2023GL103323

Received 9 MAR 2023
Accepted 16 APR 2023

Author Contributions:

Conceptualization: Eduardo Utrabo-Carazo
Data curation: Eduardo Utrabo-Carazo
Formal analysis: Eduardo Utrabo-Carazo
Funding acquisition: Cesar Azorin-Molina, Enric Aguilar, Manola Brunet
Investigation: Eduardo Utrabo-Carazo
Methodology: Eduardo Utrabo-Carazo
Project Administration: Cesar Azorin-Molina
Resources: Eduardo Utrabo-Carazo, Cesar Azorin-Molina, Enric Aguilar, Manola Brunet
Software: Eduardo Utrabo-Carazo

Abstract This study analyses for the first time observed surface mean wind speed (SWS) and gusts over the Iberian Peninsula (IP) in the frequency domain for 1961–2019, with the goal of exploring sources of predictability in the interannual and decadal scales. The main result is the high significant correlation between surface winds and the stratospheric polar vortex for periods close to 1 year with a time lag of about 2–3 months with respect to the antiphase, that is, a negative correlation in which the polar vortex modulates winds in the region. Furthermore, we found that the SWS and gusts are decoupled for periods between 9 and 11 years with a marked seasonal dependence in its intensity. Finally, we detected discrepancies between the spectra shown by surface winds from observations and ERA5-Land reanalysis, suggesting that simulated data do not accurately reproduce the variability of surface wind speeds.

Plain Language Summary In the climate system, there are oscillations that are repeated with specific time periods over time; the best known example is the El Niño-Southern Oscillation, which affects much of the world's climate. In this study, we apply a spectral analysis to: (a) characterize the spectrum of near-surface mean wind speed and gusts in the Iberian Peninsula; (b) relate the oscillations of both wind variables with those of other parameters of the climate system; and, (c) identify sources of predictability. The most outstanding result is the high significant correlation between the mean wind speed and gusts with the stratospheric polar vortex with a time lag of about 2–3 months. This means that with an anomalously weak (strong) polar vortex we might expect strong (weak) surface winds 2–3 months later. This study has direct socioeconomic and environmental implications for for example, wind energy production, agriculture and hydrology, pollutant dispersion, among others, as it could predict interannual- to decadal-scales wind speed behavior in the region.

1. Introduction

Although near-surface wind speed and gusts have not been studied as much as air temperature or precipitation in the context of climate change (IPCC, 2021), in recent years numerous studies have analyzed winds in the time domain, calculating their trends and correlations with different climate indices at different spatio-temporal scales (e.g., McVicar et al., 2012; Wu et al., 2018); this has also been the case for the Iberian Peninsula (IP, Azorin-Molina et al., 2014, 2016; Utrabo-Carazo et al., 2022). However, to the authors' knowledge, there is only one study in the scientific literature that analyses surface wind speed in the frequency domain (Naizghi & Ouarda, 2017) despite all the insights that can be gained from a spectral analysis approach (Grinsted et al., 2004). The study of surface winds is of great socioeconomic and environmental importance for a large number of areas, with special emphasis on the production of electrical power (Liu et al., 2022). In 2019, the installed electricity capacity of wind power corresponded to approximately 25% of the total for the IP (European Commission and Directorate-General for Energy, 2021). Therefore, the ability to predict surface winds, thus, the production of this kind of energy is essential as the principal force for decarbonization (Wu et al., 2021).

The characteristics of the spectrum of the variable to be considered allow us to recognize whether it is possible the existence of sources of predictability or if, on the contrary, its behavior is chaotic (Serykh & Sonechkin, 2019). Furthermore, techniques based on wavelets can be used to locate the main oscillations in time, allowing us to recognize non-stationary behavior (Grinsted et al., 2004). These techniques have been successfully applied to different climatic variables such as precipitation or air temperature (e.g., Penalba & Vargas, 2004; Polanco-Martínez et al., 2020). As mentioned above, spectral analysis has only been applied once to surface winds in United

Supervision: Cesar Azorin-Molina, Enric Aguilar, Manola Brunet
Validation: Eduardo Utrabo-Carazo
Visualization: Eduardo Utrabo-Carazo
Writing – original draft: Eduardo Utrabo-Carazo
Writing – review & editing: Eduardo Utrabo-Carazo, Cesar Azorin-Molina, Enric Aguilar, Manola Brunet

Arab Emirates (Naizghi & Ouarda, 2017), revealing its potential for the study of surface wind variability. Being non-linear and non-stationary, wavelet. allow to retrieve more features than classical linear analysis, such as trends or Pearson correlation (Mares et al., 2021).

The observed changes in surface wind speed are mainly driven by internal decadal ocean–atmosphere oscillations (Zeng et al., 2019), making the spectral techniques employed here a powerful tool for characterizing these relationships. In the climate system, there are oscillations that are well-known to influence weather and climate, such as the North Atlantic Oscillation (NAO, Vicente-Serrano & Trigo, 2011), the Western Mediterranean Oscillation (WeMO, Martin-Vide & Lopez-Bustins, 2006) or the El Niño-Southern Oscillation (ENSO, Rodríguez-Fonseca et al., 2016), to name but a few. Therefore, it could be possible that these oscillations are used as sources of interannual- to decadal-scales wind speed predictability. Furthermore, the stratospheric polar vortex has a high impact on the European climate in autumn, winter and spring (e.g., Smith et al., 2018). Extreme vortex events such as sudden stratospheric warmings (SSW) that occur with a certain periodicity cause noticeable effects on the weather in our study region (e.g., Ayarzagüena et al., 2018).

Up to now, the attribution of the processes behind the near-surface mean wind speed (SWS) and daily peak wind gust (DPWG) variability and change is challenging, as well as its inherent predictability. Therefore, the overall aim of this research is to apply for the first time in the IP these time-frequency analysis to observed SWS and DPWG. More specifically, particular objectives are:

1. To estimate the power spectral density of the near-SWS and DPWGs.
2. To explore possible sources of predictability for both wind variables through wavelet analysis, estimating its correlation and time lag with a set of modes of climate variability.
3. To compare between surface wind spectra from observed data and from a reanalysis.

Section 2 covers a description of the data and methods used; Section 3 presents the results; Section 4 discusses the principal findings against the state-of-the-art; and, lastly, Section 5 highlights the principal conclusions and future perspectives of this research.

2. Data and Methods

2.1. Data

The near-surface wind data (~10 m above the ground) correspond to two quality controlled and homogenized wind datasets described in Utrabo-Carazo et al. (2022); one for the monthly SWS and the other for the DPWG. Both observed wind series contain 87 meteorological stations across the IP (covering Spain and Portugal; Figure S1 in Supporting Information S1), comprising the 59-yr 1961–2019 period. The DPWG is defined as the maximum wind speed recorded as a 3-s mean over 24 hr, while SWS is the daily mean wind speed. Here we computed monthly anomaly series for SWS and DPWG with respect to the 1981–2010 period.

The zonal component of wind at 60°N and at the 10 hPa level (hereinafter Polar vortex) is selected from the ERA5 reanalysis (available online at https://www.ecmwf.int/en/forecasts/datasets/reanalysis-datasets/era5; last accessed 30 January 2023). It is chosen as a representation of the state of the polar vortex (Charlton & Polvani, 2007). Again, the monthly anomaly series is computed.

In this study, ocean-atmosphere oscillations are represented by three climate indices: (a) the Niño 3.4 SST Index (Niño 3.4) is retrieved from the National Oceanic and Atmospheric Administration (NOAA; available online at https://psl.noaa.gov/gcos_wgsp/Timeseries/Nino34; last accessed 30 January 2023), it is chosen due to the influence of ENSO on the North Atlantic region (Rodríguez-Fonseca et al., 2016; Taschetto et al., 2020); (b) the NAO index (NAOi; available online at https://crudata.uea.ac.uk/cru/data/nao/; last accessed 30 January 2023); and (c) the Western Mediterranean Oscillation index (WeMOi; available online at http://www.ub.edu/gc/es/wemo/; last accessed 30 January 2023). NAOi and WeMOi are chosen due to their proven high significant correlation with both SWS and DPWG over the IP, negative for NAOi and positive for WeMOi (Azorin-Molina et al., 2014, 2016; Utrabo-Carazo et al., 2022).

Finally, since reanalyzes fail to accurately reproduce the change and variability of near-surface wind speed (Ramon et al., 2019), we evaluate whether the spectra of one of them differs from the observed data, which would imply that it indeed exhibits different climate variability. We use the u and v components of the 10 m wind averaged over the entire IP (i.e., approximately, from 9.5°W to 3.3°E and from 36.0°N to 43.8°N) of the ERA5-Land reanalysis data set (Muñoz Sabater, 2021) to compare the near-surface wind speed wavelet spectra from observed versus reanalysis datasets, as well as the wavelet coherence (WC) with other climate parameters. ERA5 at 31 km has been assessed as the

best reanalysis in reproducing near-surface wind speed (Ramon et al., 2019). Due to the higher resolution of ERA5-Land at 9 km, we expect a better representation of near-surface wind speed and therefore has been chosen in this study.

2.2. Methods

Here we apply two different approaches to characterize the parameters defined above in the frequency domain: (a) the power spectral density is obtained through the multitaper method (Thomson, 1982) using the MATLAB toolbox "jLab" (available online at http://jmlilly.net/software.html; last accessed 30 January 2023). This technique better estimates the spectrum compared to the conventional Fourier analysis since multiple independent estimates of the spectrum are obtained from the same sample (Bronez, 1992; Percival & Walden, 1993). We choose the seven lowest-order Slepian orthogonal tapers of length 708 (total number of months in the series) and time-bandwidth product seven to calculate the multitaper power spectrum density. For comparison, we will also calculate the Fourier power spectrum as well as the theoretical noise spectrum (considering red noise) with a significance level of 0.95. For both spectral estimations the data will be detrended and normalized by its standard deviation; and (b) the wavelet analysis is performed through the MATLAB toolbox "Cross wavelet and WC" (available online at https://github.com/grinsted/wavelet-coherence; last accessed 30 January 2023). We chose the Morlet wavelet with six as the dimensionless frequency as the mother wavelet, 2 months as the starting scale, 12 sub-octaves per octave and 84 as the total number of scales. More information about the meaning of these elections can be found at Torrence and Compo (1998), Grinsted et al. (2004), and Naizghi and Ouarda (2017). We will compute: (a) the Continuous Wavelet transform (CWT) of each variable defined above, and (b) the WC between the wind variables and the rest of the parameters. The definition of the cone of influence (COI), a region where edge effects cannot be ignored, and of the test to estimate the statistical significance of the wavelet power against a red noise spectrum can be found at Grinsted et al. (2004). Red noise is characteristic of weather signals, it has a higher spectral density at low frequencies than at high frequencies indicating a high autocorrelation, unlike white noise where the power is equally distributed at all frequencies (Gilman et al., 1963). The power represented in the CWT figures is normalized by the variance of the parameter considered and is therefore dimensionless, so that the different spectra can be compared. The arrows in the WC analysis indicate the relative phase between the two variables to be analyzed, which in turn is related to the time lag between them. In the case of a cause and effect mechanism, we would expect the arrows to point in the same direction throughout the time series for a given period. When estimating the time lag we must be cautious; for example, arrows pointing to the right could indicate that both signals are in phase or that there is 180° with respect to the antiphase, and so on. Therefore, additional information about the underlying mechanisms is needed to accurately determine the time lag from the phase arrows. For a specific period, the time lag can be approximated as the phase angle times the period divided by two times π. For more information about wavelet analysis see Torrence and Compo (1998) and the references therein.

3. Results

3.1. Power Spectral Density

Figure 1 shows the power spectral density calculated for all the parameters defined in Section 2.1, both from the Fast Fourier Transform and multitaper method. It can be seen the red noise which is characteristic of climate signals, with the power increasing as the frequency goes down, being more prominent in the Niño 3.4 spectrum. In all cases, it is discernible a transition from a continuous spectrum for periods of less than a year approximately, to a spectrum that tends to be more discrete for longer periods. At the low-frequency part of the spectrum, significant regions for both NAOi and WeMOi appear in periods longer than 8 years, with the significant region for El Niño3.4 occurring between 1 and 6 years. However, for the polar vortex no region is significant except for the seasonal cycle. The significant region at the lower frequency end for the SWS and DPWG anomalies could be associated with trends that have not been eliminated by the linear detrend.

3.2. Continuous Wavelet Transform

The CWT of all variables are shown in Figure 2. The results for the SWS anomalies (a) and for the DPWG anomalies (b) show quite similarity. The most powerful and statistically significant regions are located in periods between 8 and 16 months, although there are non-significant regions with high relative power for longer periods. As for SWS and DPWG anomalies, (c) the Polar vortex concentrates all its significant power in the periods between 8 and 16 months but unlike before, no other regions with high relative power are found. In contrast

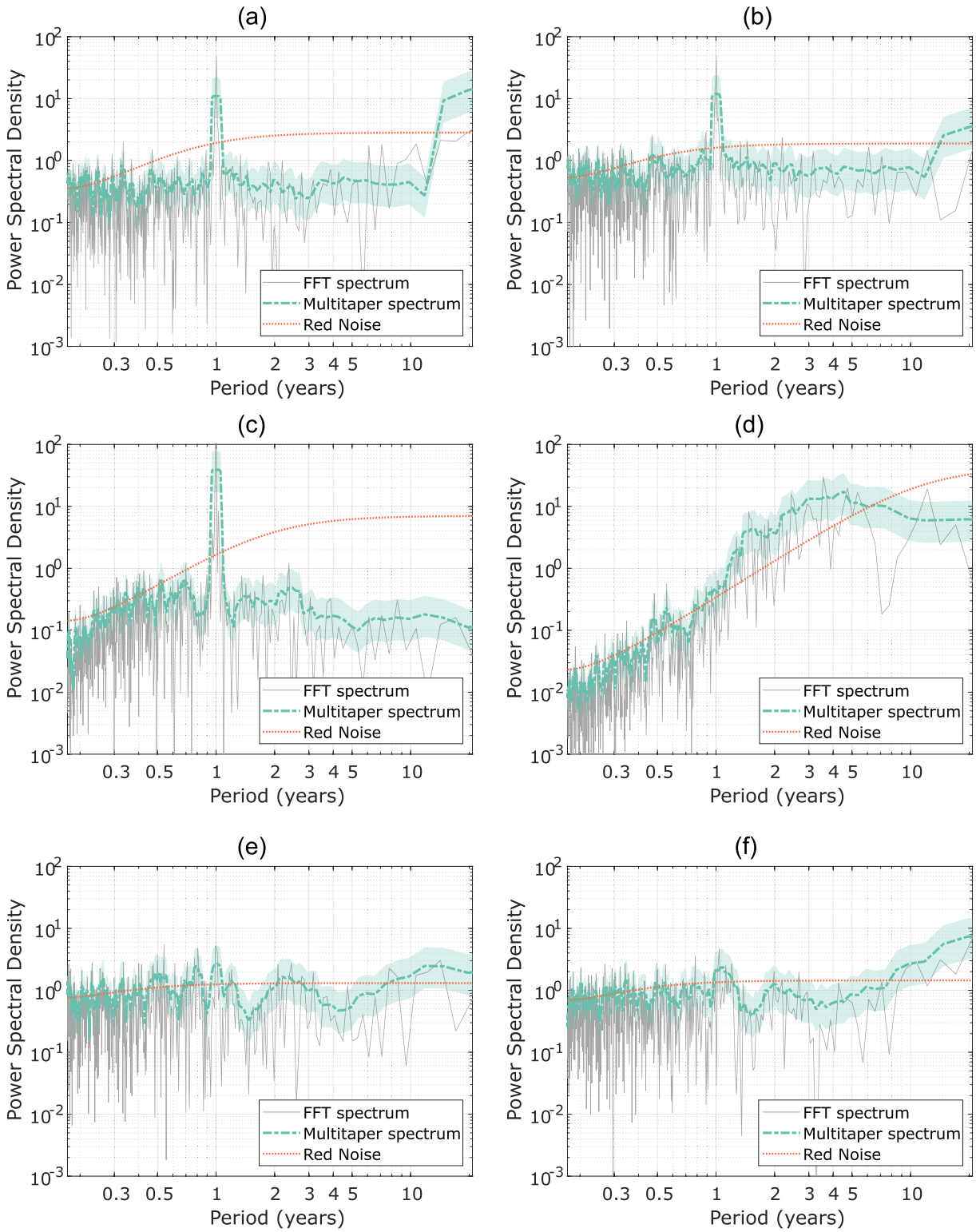

Figure 1. Power Spectral Density of detrended and normalized: (a) Surface mean wind speed anomalies, (b) daily peak wind gust anomalies, (c) Polar vortex, (d) Niño 3.4, (e) North Atlantic Oscillation index and (f) Western Mediterranean Oscillation index. The red dotted line correspond to the theoretical red noise spectra, the gray line correspond to the spectrum calculated from Fast Fourier Transform (FFT), the blue dash-dotted line correspond to the spectrum calculated from Multitaper method and the light blue area correspond to the 95% confidence interval.

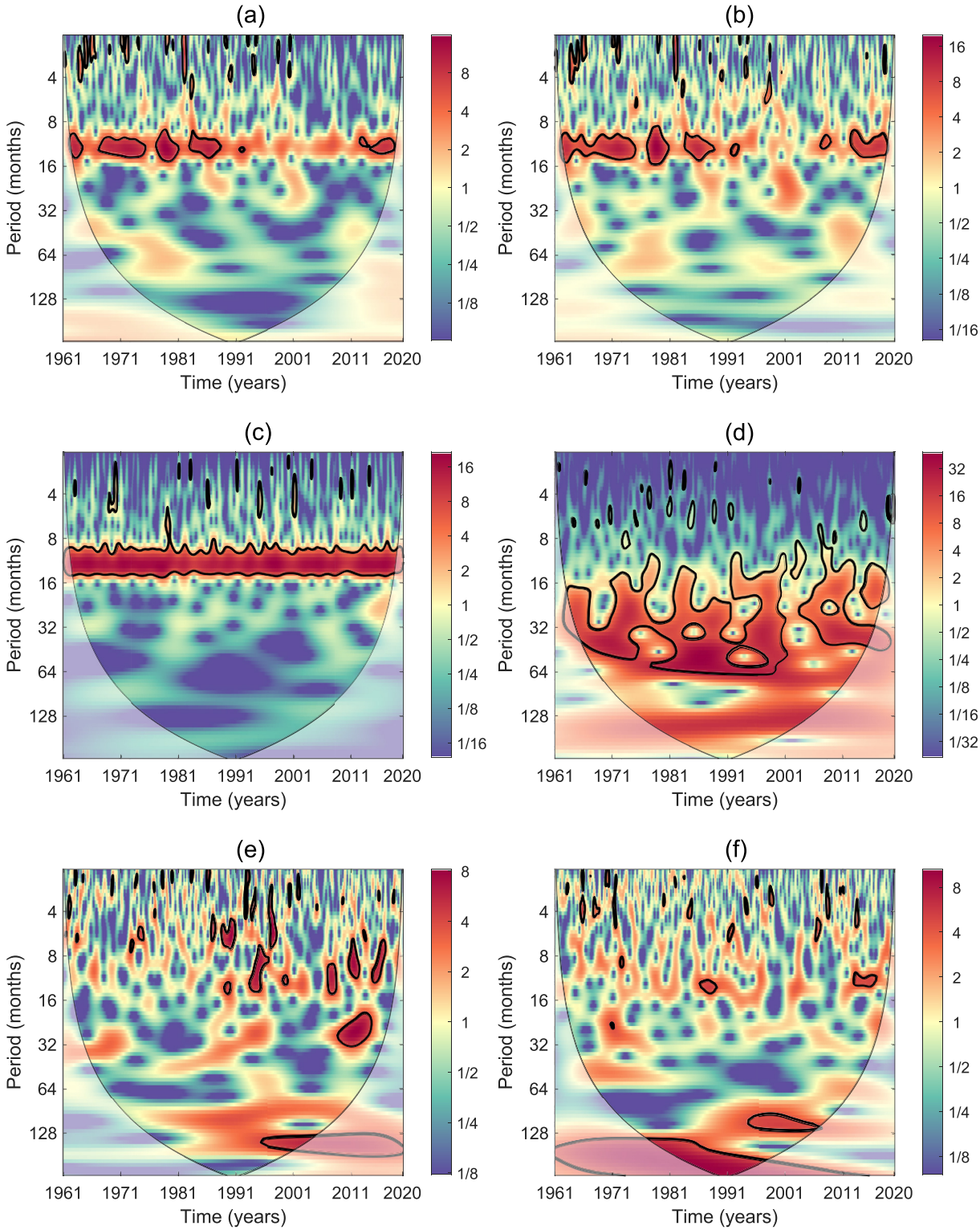

Figure 2. Continuous Wavelet Transform of: (a) Surface mean wind speed anomalies, (b) daily peak wind gust anomalies, (c) Polar vortex, (d) Niño 3.4, (e) North Atlantic Oscillation index, and (f) Western Mediterranean Oscillation index. The thick black contour designates the significant regions against red noise ($p < 0.05$) and the cones of influence (COI) where edge effects might distort the results are shown as a lighter shade.

to these variables, (d) the Niño 3.4 shows a high generalized power in all periods longer than approximately 12 months, with the statistically significant region between 12 and 64 months. Finally, the results for (e) the NAOi and (f) the WeMOi show a greater temporal discontinuity, with the regions with the highest power gathered at certain points in time. For the NAOi, there is a statistically significant region around 2011 with periods between 16 and 32 months, and a region with a period longer than 128 months starting around 1994. For the WeMOi, there is a significant region for periods longer than 130 months, but the series is too short and most of it falls within the COI, and there is also a significant region between 1994 and 2008 for periods close to 120 months.

3.3. Wavelet Coherence

Looking at the WC between both SWS (Figure 3) and DPWG (Figure S2 in Supporting Information S1) anomalies and the rest of the parameters, the most outstanding result corresponds to the high correlation with the Polar vortex for periods ranging from 8 to 16 months with an approximate relative phase of 60° for SWS and 80° for DPWG with respect to the antiphase. This means that when the Polar vortex is weak, strong winds occur 2 months later for SWS and 2.5 months later for DPWG across the IP; the opposite for strong Polar vortex events. Other signals among these variables are found in the periods between 70 and 100 months, being significant and approximately in phase at the beginning of the series between 1961 and 1981. Here we also find that SWS and DPWG are decoupled for periods between 9 and 11 years, meaning that there is no correlation between them. For the rest of the periods, these variables are coupled, which means that the correlation is significant, high and in phase, as expected for these two variables. Moreover, the correlations between the wind variables and the rest of the climate indices (i.e., Niño 3.4, NAOi, and WeMOi) show a nearly non-stationary behavior, that is, the main statistically significant signals vary with time. In the case of the NAOi, the correlation observed between 1991 and 2011 around the frequency of 64 months for both SWS and DPWG anomalies is noteworthy. For the Niño 3.4, the highest and significant correlations are found in two period bands, 16–32 months and 64–100 approximately, and in two time periods, 1961–1976 and 2001–2019, with the former being of greater magnitude for SWS anomalies and the latter for DPWG anomalies. A large part of these bands are within the COI, so their reliability is not too high. Finally, the correlations with the WeMOi are the most widespread among these three modes of climate variability. They are distributed in patches between 8 and 128 months and during the entire time interval. The region between 64 and 100 months from 2001 onwards stands out, which could be related to that observed in the case of the Niño 3.4, being again of greater extension for the DPWG anomalies.

On a seasonal scale, the decoupling between SWS and DPWG tend to occur in the warm period of the year (Figures S3–S10 in Supporting Information S1), starting in spring, being of greater magnitude in summer, approaching coupling in autumn and both variables being fully coupled in winter. As expected, the correlation with the NAOi increases in winter, being significant in most of the time series and in almost all periods. Another noticeable seasonal result is the high significant correlation between DPWG and the Niño3.4 in autumn for periods around 15 years; this result could indicate that the most extreme ENSO events, whose period is close to those 15 years, could have a great impact on the IP.

3.4. Differences With ERA5-Land Spectra

There are differences between the spectra of the observed data and those from the ERA5-Land reanalysis. In general, the power spectral density is higher at all scales for the series from the reanalysis (Figure S11 in Supporting Information S1), indicating that the variability of this parameter differs between the observations and the reanalysis, the latter being more predictable. The CWT does not show such a marked seasonal cycle in the case of the reanalysis; moreover, it presents a statistically significant region at the beginning of the series in periods around 32 months that does not appear in the observed data (Figure S12 in Supporting Information S1). The WC (Figure 4) confirms these differences, there are large regions where there is no correlation between the wind anomalies from the reanalysis and the SWS and DPWG from the observations, even with a slight time lag in some cases. The correlation with the Polar vortex is also weaker and, in this case, the approximate relative phase is 130° and the time lag is about 4 months. Both the correlation with the Niño 3.4 and with the NAOi are also lower than for the observations. The only correlation that is higher is with the WeMOi.

4. Discussion

A time-frequency analysis of observed SWS and DPWG has been applied for the first time in the IP and, as far as we know, for the second time worldwide (Naizghi & Ouarda, 2017). The power spectral density and wavelet

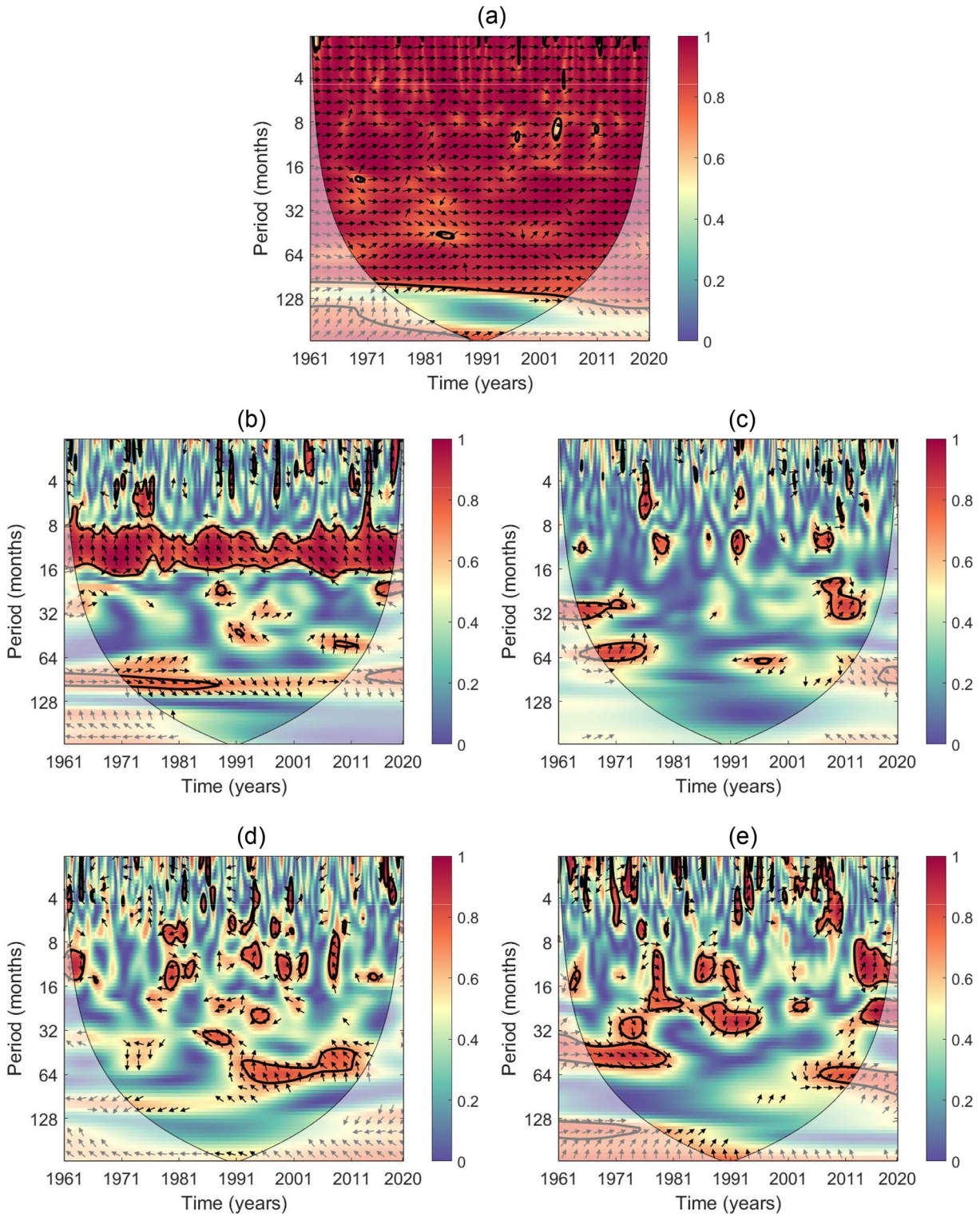

Figure 3. Wavelet coherence between surface mean wind speed (SWS) anomalies and: (a) daily peak wind gust anomalies, (b) Polar vortex, (c) Niño 3.4, (d) North Atlantic Oscillation index, and (e) Western Mediterranean Oscillation index. The thick black contour designates the significant regions against red noise ($p < 0.05$) and the cones of influence (COI) where edge effects might distort the results are shown as a lighter shade. The relative phase relationship is shown as arrows, with in-phase pointing right, anti-phase pointing left, and SWS anomalies leading the other variable by 90° pointing straight down.

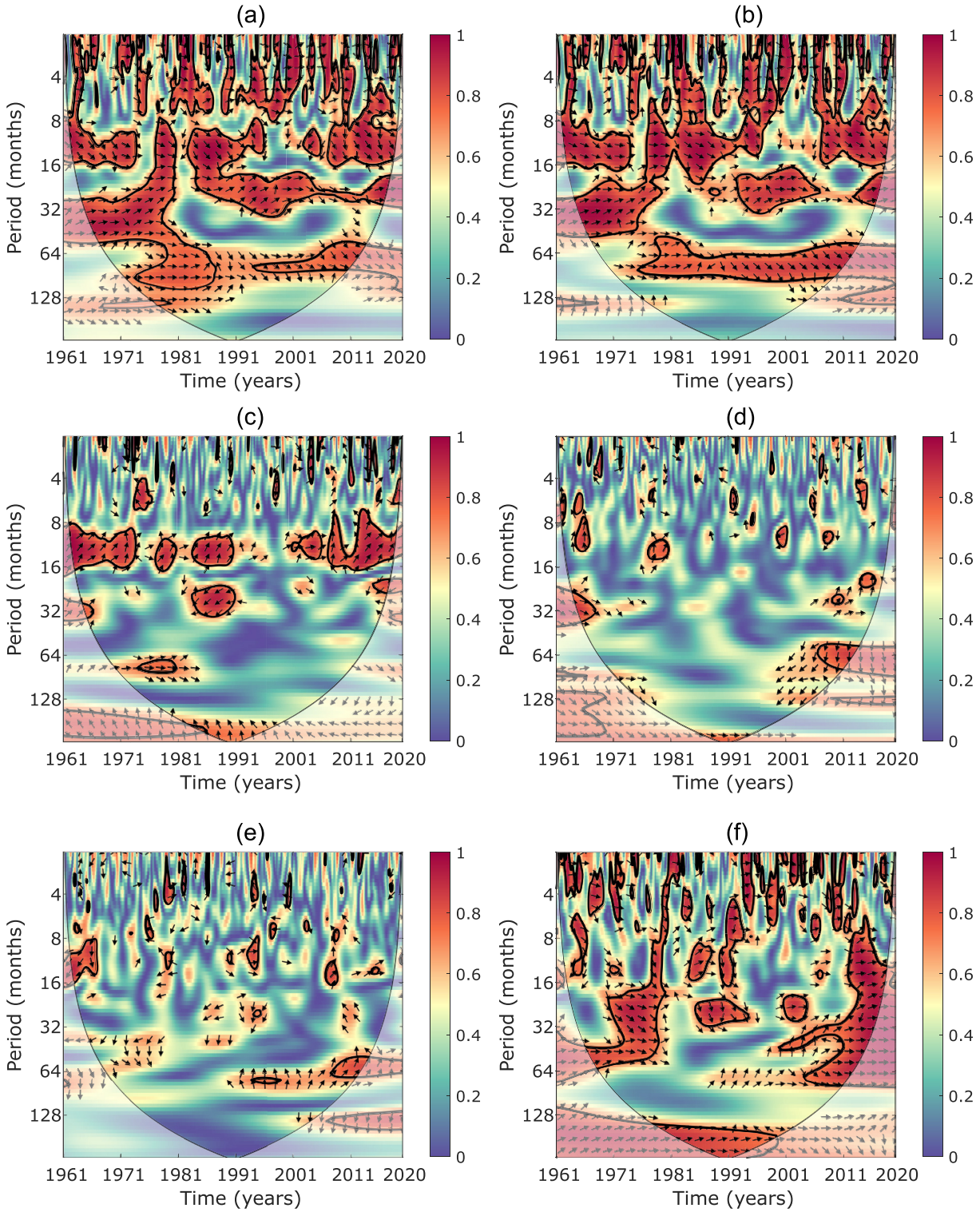

Figure 4. Wavelet coherence between surface mean wind speed (SWS) anomalies from ERA5-Land and: (a) SWS anomalies from observations, (b) daily peak wind gust (DPWG) anomalies, (c) Polar vortex, (d) Niño 3.4, (e) North Atlantic Oscillation index, and (f) Western Mediterranean Oscillation index. The thick black contour designates the significant regions against red noise ($p < 0.05$) and the cones of influence (COI) where edge effects might distort the results are shown as a lighter shade. The relative phase relationship is shown as arrows, with in-phase pointing right, anti-phase pointing left, and DPWG anomalies leading the other variable by 90° pointing straight down.

analysis are used here to obtain sources of predictability in the interannual- to decadal-scales. Previous studies have focused on analyzing these variables in the time domain, obtaining that one of the main causes of the observed changes is partly driven by internal ocean–atmosphere oscillations (e.g., Zeng et al., 2019). Therefore, a next logical step on the assessment and attribution of wind changes was to study these oscillations by means of spectral techniques, which provides a robust framework in which to characterize periodic signals (Dillon et al., 2016; Wang & Dillon, 2014). It is necessary to have sufficiently long series in order to apply this kind of analysis to the scales we are considering (Torrence & Compo, 1998). This is sometimes difficult for atmospheric and climate sciences and even more for SWS and DPWG (Azorin-Molina et al., 2014), which would explain why they have not been applied before.

Results of the spectral power density estimation reinforce the feasibility of obtaining predictability sources for SWS and DPWG on scales longer than 1 year, when there is a transition from chaotic to quasi-periodic behavior. This finding had already been explored for another set of climatic variables by Serykh and Sonechkin (2019). The differences between the spectra of the selected variables indicate that some show greater periodicity than others. For example, the stratospheric polar vortex forms every year in autumn and disappears in spring (Waugh et al., 2017), so its annual signal is the largest of those analyzed. The highest power bands for the Niño3.4 in the CWT, between 1 and 6 years, match previous results (Hope et al., 2017).

The seasonal cycle is the strongest signal in both wind variables due to the extratropical location of the IP and the influence of different atmospheric dynamics throughout the year. If we compare the wavelet spectra of the wind variables for the IP with those for the United Arab Emirates (Naizghi & Ouarda, 2017), the annual cycle is quite similar, however, the biannual periodicity is not observed in the IP. The WC spectra with the NAOi and the Niño3.4 are different for both, probably because its different location, which influence the correlations with both teleconnection patterns. As mentioned in Section 3.3, the correlations are non-stationary with these indexes. This result was previously found for WC between hydrological time series and the NAOi in Portugal (Neves et al., 2019) and in the IP as a whole (Merino et al., 2015). In line with these findings, the relationship between the NAOi and the SWS and DPWG in winter (Figures S3 and S7 in Supporting Information S1) is in antiphase (i.e., arrows toward 180°), which might indicate a negative linear correlation in agreement with Utrabo-Carazo et al. (2022). Likewise, for the Niño3.4 index, previous results indicate that the impact of this climatic pattern in Europe is non-linear and non-stationary for both air temperature (Martija-Díez et al., 2021) and precipitation (Martija-Díez et al., 2022), showing a seasonal dependence in western Europe (Shaman, 2014). The only exception for a non-stationarity behavior found here occurred in autumn for the DPWG in periods longer than 8 years when this signal lasted all 59 years of study. This could indicate that extreme ENSO events (Wang et al., 2017) might produce a signal in the DPWG over the IP regardless of the previous conditions in the region.

The spectrum of the WC between the polar vortex and the two wind variables would agree with what we know about SSW and their effects on the troposphere, since a SSW with a tropospheric signal would translate into a negative NAO (Hall et al., 2021). This NAO phase negatively correlates with SWS and DPWG over the IP (Utrabo-Carazo et al., 2022). The time it takes for the SSW signal to reach the troposphere varies from one event to another, sometimes not occurring at all (Hall et al., 2021); the 2–3 months of time lag found here might correspond to the average of all the events that occurred in the studied period. However, it is noteworthy that this correlation at scales around the year was not found between NAOi and SWS and DPWG. Recent studies show that although NAOi is indeed sensitive to the state of the stratospheric polar vortex, this does not mean that we should always expect a negative NAO after a SSW (Beerli & Grams, 2019; Charlton-Perez et al., 2018). This would indicate that there are other mechanisms, besides the NAOi, by which the stratospheric polar vortex would affect the surface wind speed over the IP.

The decoupling between the SWS and DPWG, since it occurs in the warm months and not in winter, could be due to the different mechanisms behind extreme winds over the region (Gayà, 2011). On the one hand, in winter, the synoptic scale is predominant, with cold fronts regularly passing, causing strong SWS and DPWG or days dominated by blocking anticyclonic weather type with weak SWS and DPWG. On the other hand, in summer, the atmospheric stability dominates but some extreme local to mesoscale events of short duration, such as downbursts (Bolgiani et al., 2020), can produce strong DPWG without this being reflected in the SWS. The different mechanisms behind mean and extreme winds could explain the decoupling, but not the fact that they occur in periods between 9 and 11 years. The unavailability of daily mean wind speed data limits the possibility of testing this hypothesis. It is noteworthy to mention that here we analyzed time series of 59 years, which would only

contain 5 complete cycles of oscillations with a period of 11 years. Therefore, the power associated with this period could be due to chance and not to specific physical mechanisms. Furthermore, since the wavelets are localized in time edge effects can distort the results, hence the inclusion of the COI, so that only oscillations occurring in the middle of the series are taken into account here. Lastly, long periods in relatively short series could be mistaken for trends, so the decoupling could be due to differences in magnitude between DPWG and SWS trends (Utrabo-Carazo et al., 2022); although we have repeated the wavelet analyses eliminating the linear trend (not shown) and the results are similar.

The discrepancies found between the wavelet spectra for SWS observations and ERA5-Land reanalysis might be due to the fact that the reanalyzes do not accurately reproduce wind observations (Ramon et al., 2019). It is also noteworthy that the time lag with the polar vortex is different for both datasets, being greater in the case of the reanalysis. Probably because the reanalysis is not correctly reproducing the SSWs or the arrival of its signal to the troposphere. The complexity of SSWs produces uncertainty about the mechanisms behind this phenomenon and their consequences in the troposphere (Hall et al., 2021). Therefore, it is expected that current models and reanalyzes are not able to simulate with accuracy the effects of SSWs on surface weather, particularly for SWS and DPWG (Baldwin et al., 2021).

The next steps on this research will be to analyze the influence of other phenomena such as the quasi-biennial oscillation or the AMOC, and to determine the mechanisms that drive the relationships found here. Moreover, the wavelet analysis techniques could be applied in a multivariate manner (Polanco-Martínez et al., 2020) or even by applying bandpass filters to increase the signal-to-noise ratio at the desired frequencies (Mares et al., 2021). Much longer time observed SWS and DPWG series will be needed to detect signals in the long term. Furthermore, it is also necessary to extend the analyses to other locations in the Northern Hemisphere to confirm these results and examine possible variations in the influence of the polar vortex at different latitudes. In addition, since wind speed is highly dependent on local scale phenomena, these analyses could be performed for each station individually or by applying a clustering that classifies stations according to common dynamic characteristics.

The results found here could have great impact in air quality (Wu et al., 2018), fishing industry (Kahru et al., 2010), and especially in the wind energy industry (Tian et al., 2019) since it might allow to predict the power generated by wind farms in the region in the interannual- to decadal-scales. Finally, spectral analysis techniques can serve to estimate wind climate conditions several months in advance, with adequate sampling frequency these techniques could be of great applicability for seasonal and sub-seasonal wind forecasting (Lledó et al., 2019), as well as to the study of extreme wind events such as wind droughts (Lledó et al., 2018). This is crucial for decision makers in order to reduce the socioeconomic and environmental implications of weak or strong wind conditions, and to establish short-term adaptation to wind change and variability (He et al., 2021).

5. Conclusions

The main findings of this research can be summarized as follows: (a) The WC analysis found a high and significant correlation between the stratospheric polar vortex and the near-SWS and DPWGs anomalies in periods close to the year, with a time lag of two-three months with respect to the antiphase, that is the polar vortex correlates negatively with surface winds. (b) There is a decoupling between SWS and DPWG anomalies for periods between 9 and 11 years and significant, high and in phase correlation for the rest of the periods; this decoupling disappears in winter and it is stronger in summer. (c) There are differences in CWT and WC spectra between observed and ERA5-Land reanalysis surface winds; indicating that the SWS variability of the reanalysis is different from that of the observations.

Data Availability Statement

The SWS and DPWG monthly anomaly series can be found at Utrabo-Carazo (2023) (https://doi.org/10.5281/zenodo.7714008; last accessed 8 March 2023). The NAO index was retrieved from CRU (https://crudata.uea.ac.uk/cru/data/nao/; last accessed 30 January 2023), the WeMO index was downloaded from the Climatology Group of the University of Barcelona (http://www.ub.edu/gc/es/wemo/; last accessed 30 January 2023), the Niño 3.4 index was downloaded from NOAA (https://psl.noaa.gov/gcos_wgsp/Timeseries/Nino34; last accessed 30 January 2023). ERA5 and ERA5-Land Reanalysis data were downloaded from ECMWF (http://doi.org/10.24381/cds.adbb2d47 and https://doi.org/10.24381/cds.68d2bb30; last accessed 8 March 2023).

Acknowledgments
E. U.-C. was supported by the FPI fellowship (PRE2019-090148). This study was conducted in the framework of the IBER-STILLING project RTI2018-095749-A-100 (MCIU/AEI/FEDER,UE); the VENTS project (GVA-AICO/2021/023); the RED-CLIMA project (LINCGLOBAL-CSIC, INCGLO0023); the CSIC Interdisciplinary Thematic Platform (PTI) Clima (PTI-CLIMA); and the "*Unidad Asociada CSIC-Universidad de Vigo: Grupo de Física de la Atmosfera y del Océano*." We acknowledge the two anonymous reviewers for their detailed and helpful comments to the original manuscript.

References

Ayarzagüena, B., Barriopedro, D., Garrido-Perez, J., Abalos, M., de la Cámara, A., García-Herrera, R., et al. (2018). Stratospheric connection to the Abrupt end of the 2016/2017 Iberian drought. *Geophysical Research Letters*, *45*(22), 12639–12646. https://doi.org/10.1029/2018GL079802

Azorin-Molina, C., Guijarro, J. A., McVicar, T. R., Vicente-Serrano, S. M., Chen, D., Jerez, S., & Espirito-Santo, F. (2016). Trends of daily peak wind gusts in Spain and Portugal, 1961–2014. *Journal of Geophysical Research: Atmospheres*, *121*(3), 1059–1078. https://doi.org/10.1002/2015JD024485

Azorin-Molina, C., Vicente-Serrano, S. M., McVicar, T. R., Jerez, S., Sanchez-Lorenzo, A., López-Moreno, J. I., et al. (2014). Homogenization and assessment of observed near-surface wind speed trends over Spain and Portugal, 1961–2011. *Journal of Climate*, *27*(10), 3692–3712. https://doi.org/10.1175/JCLI-D-13-00652.1

Baldwin, M. P., Ayarzagüena, B., Birner, T., Butchart, N., Butler, A. H., Charlton-Perez, A. J., et al. (2021). Sudden stratospheric warmings. *Reviews of Geophysics*, *59*(1), e2020RG000708. https://doi.org/10.1029/2020RG000708

Beerli, R., & Grams, C. M. (2019). Stratospheric modulation of the large-scale circulation in the Atlantic–European region and its implications for surface weather events. *Quarterly Journal of the Royal Meteorological Society*, *145*(725), 3732–3750. https://doi.org/10.1002/qj.3653

Bolgiani, P., Fernández-González, S., Valero, F., Merino, A., García-Ortega, E., Sánchez, J. L., & Martín, M. L. (2020). Simulation of atmospheric microbursts using a numerical mesoscale model at high spatiotemporal resolution. *Journal of Geophysical Research: Atmospheres*, *125*(4), e2019JD031791. https://doi.org/10.1029/2019JD031791

Bronez, T. (1992). On the performance advantage of multitaper spectral analysis. *IEEE Transactions on Signal Processing*, *40*(12), 2941–2946. https://doi.org/10.1109/78.175738

Charlton, A. J., & Polvani, L. M. (2007). A new look at stratospheric sudden warmings. Part I: Climatology and modeling benchmarks. *Journal of Climate*, *20*(3), 449–469. https://doi.org/10.1175/JCLI3996.1

Charlton-Perez, A. J., Ferranti, L., & Lee, R. W. (2018). The influence of the stratospheric state on North Atlantic weather regimes. *Quarterly Journal of the Royal Meteorological Society*, *144*(713), 1140–1151. https://doi.org/10.1002/qj.3280

Dillon, M. E., Woods, H. A., Wang, G., Fey, S. B., Vasseur, D. A., Telemeco, R. S., et al. (2016). Life in the frequency domain: The biological impacts of changes in climate variability at multiple time scales. *Integrative and Comparative Biology*, *56*(1), 14–30. https://doi.org/10.1093/icb/icw024

European Commission and Directorate-General for Energy. (2021). *EU energy in figures: Statistical pocketbook 2021*. Publications Office of the European Union. https://doi.org/10.2833/511498

Gayà, M. (2011). Tornadoes and severe storms in Spain. *Atmospheric Research*, *100*(4), 334–343. https://doi.org/10.1016/j.atmosres.2010.10.019

Gilman, D. L., Fuglister, F. J., & Mitchell, J. M. (1963). On the power spectrum of "red noise". *Journal of the Atmospheric Sciences*, *20*(2), 182–184. https://doi.org/10.1175/1520-0469(1963)020<0182:OTPSON>2.0.CO;2

Grinsted, A., Moore, J. C., & Jevrejeva, S. (2004). Application of the cross wavelet transform and wavelet coherence to geophysical time series. *Nonlinear Processes in Geophysics*, *11*(5/6), 561–566. https://doi.org/10.5194/npg-11-561-2004

Hall, R., Mitchell, D., Seviour, W., & Wright, C. (2021). Tracking the stratosphere-to-surface impact of sudden stratospheric warmings. *Journal of Geophysical Research: Atmospheres*, *126*, e2020JD033881. https://doi.org/10.1029/2020JD033881

He, Y., Wu, B., He, P., Gu, W., & Liu, B. (2021). Wind disasters adaptation in cities in a changing climate: A systematic review. *PLoS One*, *16*(3), e0248503. https://doi.org/10.1371/journal.pone.0248503

Hope, P., Henley, B. J., Gergis, J., Brown, J., & Ye, H. (2017). Time-varying spectral characteristics of ENSO over the Last Millennium. *Climate Dynamics*, *49*(5–6), 1705–1727. https://doi.org/10.1007/s00382-016-3393-z

IPCC. (2021). *Climate change 2021: The physical science basis*. Cambridge University Press. https://doi.org/10.1017/9781009157896

Kahru, M., Gille, S. T., Murtugudde, R., Strutton, P. G., Manzano-Sarabia, M., Wang, H., & Mitchell, B. G. (2010). Global correlations between winds and ocean chlorophyll. *Journal of Geophysical Research*, *115*(C12), C12040. https://doi.org/10.1029/2010JC006500

Liu, Y., Zeng, Z., Xu, R., Ziegler, A. D., Jerez, S., Chen, D., et al. (2022). Increases in China's wind energy production from the recovery of wind speed since 2012. *Environmental Research Letters*, *17*(11), 114035. https://doi.org/10.1088/1748-9326/ac9cf4

Lledó, L., Bellprat, O., Doblas-Reyes, F. J., & Soret, A. (2018). Investigating the effects of Pacific Sea surface temperatures on the wind drought of 2015 over the United States. *Journal of Geophysical Research: Atmospheres*, *123*(10), 4837–4849. https://doi.org/10.1029/2017JD028019

Lledó, L., Torralba, V., Soret, A., Ramon, J., & Doblas-Reyes, F. (2019). Seasonal forecasts of wind power generation. *Renewable Energy*, *143*, 91–100. https://doi.org/10.1016/j.renene.2019.04.135

Mares, I., Dobrica, V., Mare, C., & Demetrescu, C. (2021). Assessing the solar variability signature in climate variables by information theory and wavelet coherence. *Scientific Reports*, *11*, 11337. https://doi.org/10.1038/s41598-021-90044-6

Martija-Díez, M., López-Parages, J., Rodríguez-Fonseca, B., & Losada, T. (2022). The stationarity of the ENSO teleconnection in European summer rainfall. *Climate Dynamics*. https://doi.org/10.1007/s00382-022-06596-4

Martija-Díez, M., Rodríguez-Fonseca, B., & López-Parages, J. (2021). ENSO influence on western European summer and fall temperatures. *Journal of Climate*, *34*(19), 8013–8031. https://doi.org/10.1175/JCLI-D-20-0808.1

Martin-Vide, J., & Lopez-Bustins, J.-A. (2006). The Western Mediterranean oscillation and rainfall in the Iberian Peninsula. *International Journal of Climatology*, *26*(11), 1455–1475. https://doi.org/10.1002/joc.1388

McVicar, T. R., Roderick, M. L., Donohue, R. J., Li, L. T., Van Niel, T. G., Thomas, A., et al. (2012). Global review and synthesis of trends in observed terrestrial near-surface wind speeds: Implications for evaporation. *Journal of Hydrology*, *416–417*, 182–205. https://doi.org/10.1016/j.jhydrol.2011.10.024

Merino, A., López, L., Hermida, L., Sánchez, J. L., García-Ortega, E., Gascón, E., & Fernández-González, S. (2015). Identification of drought phases in a 110-year record from western Mediterranean basin: Trends, anomalies and periodicity analysis for Iberian Peninsula. *Global and Planetary Change*, *133*, 96–108. https://doi.org/10.1016/j.gloplacha.2015.08.007

Muñoz Sabater, J. (2021). *ERA5-land monthly averaged data from 1950 to present*. Copernicus Climate Change Service (C3S) Climate Data Store (CDS). https://doi.org/10.24381/cds.68d2bb30

Naizghi, M. S., & Ouarda, T. B. M. J. (2017). Teleconnections and analysis of long-term wind speed variability in the UAE. *International Journal of Climatology*, *37*(1), 230–248. https://doi.org/10.1002/joc.4700

Neves, M. C., Jerez, S., & Trigo, R. M. (2019). The response of piezometric levels in Portugal to NAO, EA, and SCAND climate patterns. *Journal of Hydrology*, *568*, 1105–1117. https://doi.org/10.1016/j.jhydrol.2018.11.054

Penalba, O. C., & Vargas, W. M. (2004). Interdecadal and interannual variations of annual and extreme precipitation over central-northeastern Argentina. *International Journal of Climatology*, *24*(12), 1565–1580. https://doi.org/10.1002/joc.1069

Percival, D. B., & Walden, A. T. (1993). *Spectral analysis for physical applications*. Cambridge University Press. https://doi.org/10.1017/CBO9780511622762

Polanco-Martínez, J. M., Fernández-Macho, J., & Medina-Elizalde, M. (2020). Dynamic wavelet correlation analysis for multivariate climate time series. *Scientific Reports*, *10*(1), 21277. https://doi.org/10.1038/s41598-020-77767-8

Ramon, J., Lledó, L., Torralba, V., Soret, A., & Doblas-Reyes, F. J. (2019). What global reanalysis best represents near-surface winds? *Quarterly Journal of the Royal Meteorological Society*, *145*(724), 3236–3251. https://doi.org/10.1002/qj.3616

Rodríguez-Fonseca, B., Suárez-Moreno, R., Ayarzagüena, B., López-Parages, J., Gómara, I., Villamayor, J., et al. (2016). A review of ENSO influence on the North Atlantic. A non-stationary signal. *Atmosphere*, *7*(7), 87. https://doi.org/10.3390/atmos7070087

Serykh, I. V., & Sonechkin, D. M. (2019). Nonchaotic and globally synchronized short-term climatic variations and their origin. *Theoretical and Applied Climatology*, *137*(3–4), 2639–2656. https://doi.org/10.1007/s00704-018-02761-0

Shaman, J. (2014). The seasonal effects of ENSO on European precipitation: Observational analysis. *Journal of Climate*, *27*(17), 6423–6438. https://doi.org/10.1175/JCLI-D-14-00008.1

Smith, K. L., Polvani, L. M., & Tremblay, L. B. (2018). The impact of stratospheric circulation extremes on minimum Arctic sea ice extent. *Journal of Climate*, *31*(18), 7169–7183. https://doi.org/10.1175/JCLI-D-17-0495.1

Taschetto, A. S., Ummenhofer, C. C., Stuecker, M. F., Dommenget, D., Ashok, K., Rodrigues, R. R., & Yeh, S.-W. (2020). Enso atmospheric teleconnections. In *El Niño southern oscillation in a changing climate* (pp. 309–335). American Geophysical Union (AGU). https://doi.org/10.1002/9781119548164.ch14

Thomson, D. (1982). Spectrum estimation and harmonic analysis. *Proceedings of the IEEE*, *70*(9), 1055–1096. https://doi.org/10.1109/PROC.1982.12433

Tian, Q., Huang, G., Hu, K., & Niyogi, D. (2019). Observed and global climate model based changes in wind power potential over the Northern Hemisphere during 1979–2016. *Energy*, *167*, 1224–1235. https://doi.org/10.1016/j.energy.2018.11.027

Torrence, C., & Compo, G. P. (1998). A practical guide to wavelet analysis. *Bulletin of the American Meteorological Society*, *79*(1), 61–78. https://doi.org/10.1175/1520-0477(1998)079<0061:APGTWA>2.0.CO;2

Utrabo-Carazo, E. (2023). SWS_DPWG-IP [dataset]. Zenodo. https://doi.org/10.5281/zenodo.7714008

Utrabo-Carazo, E., Azorin-Molina, C., Serrano, E., Aguilar, E., Brunet, M., & Guijarro, J. A. (2022). Wind stilling ceased in the Iberian Peninsula since the 2000s. *Atmospheric Research*, *272*, 106153. https://doi.org/10.1016/j.atmosres.2022.106153

Vicente-Serrano, S. M., & Trigo, R. M. (2011). *Hydrological, socioeconomic and ecological impacts of the North Atlantic Oscillation in the Mediterranean region*. Springer.

Wang, G., Cai, W., Gan, B., Wu, L., Santoso, A., Lin, X., et al. (2017). Continued increase of extreme El Niño frequency long after 1.5°C warming stabilization. *Nature Climate Change*, *7*(8), 568–572. https://doi.org/10.1038/nclimate3351

Wang, G., & Dillon, M. E. (2014). Recent geographic convergence in diurnal and annual temperature cycling flattens global thermal profiles. *Nature Climate Change*, *4*(11), 988–992. https://doi.org/10.1038/nclimate2378

Waugh, D. W., Sobel, A. H., & Polvani, L. M. (2017). What is the polar vortex and how does it influence weather? *Bulletin of the American Meteorological Society*, *98*(1), 37–44. https://doi.org/10.1175/BAMS-D-15-00212.1

Wu, J., Han, Z.-Y., Yan, Y.-P., Sun, C.-Y., Xu, Y., & Shi, Y. (2021). Future changes in wind energy potential over China using RegCM4 under RCP emission scenarios. *Advances in Climate Change Research*, *12*(4), 596–610. https://doi.org/10.1016/j.accre.2021.06.005

Wu, J., Zha, J., Zhao, D., & Yang, Q. (2018). Changes in terrestrial near-surface wind speed and their possible causes: An overview. *Climate Dynamics*, *51*(5–6), 2039–2078. https://doi.org/10.1007/s00382-017-3997-y

Zeng, Z., Ziegler, A. D., Searchinger, T., Yang, L., Chen, A., Ju, K., et al. (2019). A reversal in global terrestrial stilling and its implications for wind energy production. *Nature Climate Change*, *9*(12), 979–985. https://doi.org/10.1038/s41558-019-0622-6